CWP-098P
September 1991

The Cagniard Method in Complex Time Revisited

by

Norman Bleistein and Jack K. Cohen

Center for Wave Phenomena
Colorado School of Mines
Golden, Colorado 80401
(303)273-3557

ABSTRACT

The Cagniard-de Hoop method is ideally suited to the analysis of wave propagation problems in stratified media. The method applies to the integral transform representation of the solution in the transform variables (s, p) dual of the time and transverse distance. The objective of the method is to make the p-integral take the form of a forward Laplace transform, so that the cascade of the two integrals can be identified as a forward and inverse transform, thereby making the actual integration unnecessary. That is, the exponent, $-sw(p)$ is set equal to $-s\tau$, with τ varying from some (real) finite time to infinity. As usually presented, the p-integral is deformed onto a contour on which the exponent is real and decreases to $-\infty$ as p goes to infinity. We have found that it is often easier to introduce a complex variable τ for the exponent and carry out the deformation of contour in the complex τ-domain. In the τ-domain the deformation amounts to "closing down" the contour of integration around the real axis while taking due account of singularities off this axis.

Typically, the method is applied to an integral that represents one body wave plus other types of waves. In this approach, the saddle point of $w(p)$ that produces the body wave plays a crucial role because it is *always* a branch point of the integrand in the τ-domain integral. Furthermore, the paths of steepest *ascent* from the saddle point are always the tails of the Cagniard path along which $w(p) \to \infty$. That is, the image of the pair of steepest ascent paths in the p-domain is a double covering of a segment of the $\mathrm{Re}\,\tau$ axis in the τ-domain. The deformed contour in the p-domain will be only the pair of steepest ascent paths unless the original integrand had other singularities in the p-domain between the imaginary axis and this pair of contours. This motivates the definition of a primary p-domain—the domain between the imaginary axis and the steepest descent paths—and its image in the τ-domain—the primary τ-domain. In terms of these regions, singularities in the primary p-domain have images in the primary τ-domain and the deformation of contour onto the real axis in the τ-domain must include contributions from these singularities.

This approach to the Cagniard-de Hoop method represents a return from de Hoop's modification to Cagniard's original method, but with simplifications that make the original method more tractable and straightforward. This approach is also reminiscent of van der Waerden's approach to the method of steepest descents, which starts exactly the same way. Indeed, after the deformation of contour in the τ-domain, the user has the choice of applying asymptotic analysis to the resulting "loop" integrals (Watson's lemma) or continuing to obtain the exact, although usually implicit, time domain solution by completing the Cagniard-de Hoop analysis.

In developing the method we examine the transformation from a frequency domain representation of the solution (ω) to a Laplace representation (s). Many users start from the frequency domain representation of solutions of wave propagation problems. There are issues of movement of singularities under the transformation from ω to s to be concerned with here. We discuss this anomaly in the context of the Sommerfeld half-plane problem.

INTRODUCTION

The Cagniard-de Hoop method, or the Cagniard (1939, 1962) method as modified by de Hoop (1958), is ideally suited to the analysis of wave propagation problems in stratified media. The method applies to the integral transform representation of the solution in the transform variables (s,p) dual of the time and transverse distance, typically of the form,

$$u(r,z,s) = \int_\Gamma f(p)\exp\{-sw(p,r,z)\}\,dp, \tag{0.1}$$

with w having the form,

$$w(p,r,z) = pr + \sum_{j=1}^{J} h_j\sqrt{p_j^2 - p^2}. \tag{0.2}$$

In this equation each h_j represents the total vertical travel distance in layer j, including multiple reflection path lengths on the trajectory from the source to an observation point, (x,z). In a two-dimensional problem (x,z), $r = |x|$ denotes the transverse range and $p_j = 1/c_j$ is the slowness in that layer. In a three-dimensional problem (x,y,z), $r = \sqrt{x^2+y^2}$ and p is the component of the slowness vector which is colinear with the vector, $\boldsymbol{x} = (x,y)$. Furthermore, $p_j^2 = 1/c_j^2 + q^2$, with q the component of the slowness vector in the orthogonal direction to $\boldsymbol{x}$. The contour of integration Γ is the imaginary p-axis. The integral (0.1) is also known as a *generalized-ray wave constitutent* or, more simply, as a *generalized ray* (Spencer, 1960; Cisternas, et al., 1973).

The objective of the method is to make the *slowness* p-integral take the form of a forward Laplace transform in *time* (possibly, a sum of such transforms). Each of these will be of the form,

$$u_n(r,z,s) = \int_{\tau_n}^{\infty} f(p(\tau))\frac{dp}{d\tau}\exp\{-s\tau\}\,d\tau. \tag{0.3}$$

If this is accomplished, then the cascade of this integral with the inverse Laplace transform from s back to time t can be identified as a forward and inverse transform

pair, making the actual inversion integration unnecessary. To achieve this, the contour Γ—the imaginary axis- -is deformed onto a path of integration on which $w(p)$ in (0.1) is real and approaches infinity. Then $w(p)$ is set equal to a *real* variable τ that varies from some finite time to infinity.

Excellent expositions of the Cagniard-de Hoop method may be found in the extensive papers of A. T. De Hoop, including his thesis (1958) and his recent tutorial (1988); also, Aki and Richards (1980) and van der Hijden (1987) are important sources.

The presentation of the method often begins with a "folding over" of the contour so that one endpoint of the integral is at $p = 0$. This leads to a representation for $u(r, z, s)$ as the imaginary part of an integral in τ. In this approach the p-path contains a section of contour starting from $p = 0$ where the integrand is real, yielding a zero contribution to the final result. However, this one-sided representation is not essential to the method and we will work with the original two-sided representation allowing the upper and lower contributions to combine at the end of the analysis, in particular canceling away the initial segment just discussed. Van der Hijden is an exception; he also applies the Cagniard-de Hoop method to the integral with both endpoints at infinity as we do here, as does de Hoop on occasion.

We have found that allowing τ to have equal status with p as a *complex* variable and considering both these complex planes, as Cagniard did [and also Dix (1954) and Garvin (1956), following Cagniard], is an important analytic tool. Thus, we take full advantage of the standard p-domain analysis in locating the singularities of the integrand in (0.1), but we carry out the deformation of contour in the τ-domain, where it amounts to "closing down" the contour of integration around the real axis while taking due account of singularities off this axis. This is often far easier than finding the curves where only $\mathrm{Re}\, w$ varies, or equivalently, the curves where $\mathrm{Im}\, w$ is

constant. This deformation of contour is further facilitated by having both endpoints at infinity, rather than having one (unphysical) endpoint at the origin in p.

In this approach the saddle points of the exponent in the original integral play a crucial role because they are *always* branch points of the integrand $f(p(\tau))dp/d\tau$, in the τ-domain integral. On the other hand, we will show that the images of the branch points at $\pm p_j$ in equation (0.2) are points of analyticity of $dp/d\tau$ in the τ-domain. Furthermore, branch points of the amplitude $f(p)$ of the same order as in the exponent at any p_j are regular points of the amplitude in (0.3) in the τ-domain. Other singularities of $f(p(\tau))$ will provide corresponding singularities in the τ-domain. Thus, it is the saddle points and these other singularities that provide the important structure of the integrand in the τ-domain. The exact evaluation of the integral involves residues from the poles enclosed in the deformation process plus loop integrals around each of the branch points in the τ-domain that are encountered in the deformation process. It is the latter type of integral that leads to integrals of the form (0.3); the inverse transform of residues at the poles is more straightforward. The deformation of contour requires the estimate of the integral on a circular arc "at infinity." The estimate that this integral approaches zero with increasing radius follows from Jordan's lemma.

A particular saddle point, p_s, located on the Re p-axis plays an especially important role. Indeed, the essence of our point of view can be explained in the context of this special saddle point with the aid of Figures 0.1 and 0.2. In the former, the contour S is made up of two steepest ascent [1] paths from the saddle point p_s when $r \neq 0$. We also show the contour Γ. We will refer to the region between Γ and S as the *primary p-domain.* It will be shown that the image Γ' of Γ is the hyperbolic-like curve of Figure 0.2 and the image S' of the contour S is a semi-infinite segment of

[1] Paths of steepest ascent and descent are paths along which Re w changes maximally; they are also paths on which Im w is constant.

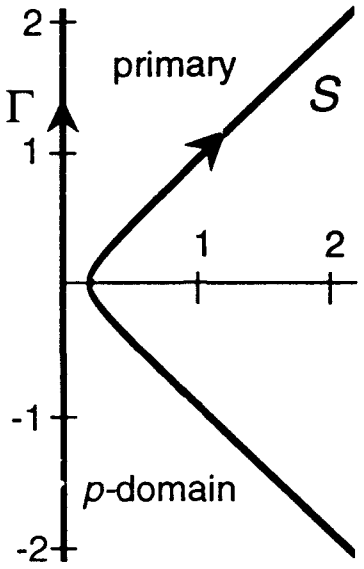

FIG. 0.1. Path Γ and steepest descent path for an example with $J = 2$, $h_1 = h_2 = 1.2$, $r = 2.5$, $1/p_1 = 3$, $1/p_2 = 4$.

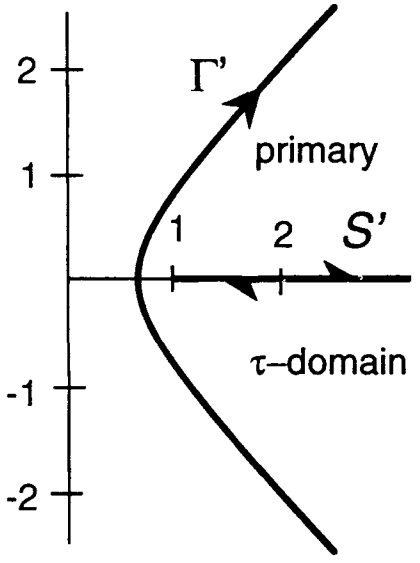

FIG. 0.2. Image contours for example of previous figure.

the real axis, doubly covered, starting from τ_s, the image of the saddle point p_s. This implies that the two steepest ascent paths which comprise S are each at least a tail of a Cagniard path. For $r \neq 0$, τ_s is to the right of the point where Γ' crosses the Re τ axis. The lower part of S maps onto the real axis, "below" a branch cut from τ_s to ∞ with $\arg(\tau_s - \tau) = \pi$ here; the upper part of S maps onto the real axis, "above" a branch cut from τ_s to ∞ with $\arg(\tau_s - \tau) = -\pi$ here. The image of the primary p-domain is the region between Γ' and S' in the τ domain. We will call this region the *primary τ-domain.* We remark that in this region $|\arg(\tau_s - \tau)| < \pi$.

Finding the p-path along which $w(r, z, p)$ is real and approaches $+\infty$, is equivalent to closing the contour Γ' down around the real axis in the τ-domain. If there are no complex singularities of the integrand, $f(p(\tau))dp/d\tau$, in the primary τ-domain then we replace Γ' by S'. The integrals above and below the cut are two integrals of the type (0.3), with two different branches of the function $p(\tau)$ taken in each integral. Typically this amounts to taking one or the other sign of a square root. In this case, the two steepest ascent paths comprising S are the Cagniard paths for two semi-infinite integrals whose form in the τ-domain is exactly (0.3). From the method used to arrive at the deformed paths as segments of S', it is clear how to deal with the singularities on the real τ axis: the contour of integration passes *above* such a singularity on the upper part of the path S' and passes *below* such a singularity on the lower part of the path S'.

If there are singularities in the primary τ-domain, then one must take account of them in carrying out the deformation of contour. However, singularities in the primary τ-domain are the images of singularities in the primary p-domain. Thus, we can find these singularities in the p-plane, which is often easier. Furthermore, we can be sure that singularities to the left of the primary p-domain are also to the left of the primary τ-domain and have no effect on the contour deformation

process. Somewhat similarly, singularities to the *right* of the primary p-domain are also outside the primary τ-domain. They lie in the region where $|\arg(\tau_s - \tau)| > \pi$, usually described as being on a "second Riemann sheet" of the τ-domain. While they do not obstruct the deformation of contour from Γ' to S', they can be close enough to S' that their "influence" is felt in the integration along S'. Examples of this type are discussed in the above cited literature.

We have twice included the caveat $r \neq 0$. The case $r = 0$ is degenerate; $\Gamma = S$ and the primary p-domain collapses to the imaginary axis with its image being the right half $\mathrm{Re}\,\tau$ axis, starting from $\tau_s = \tau(p = 0)$, doubly covered just as in Figure 0.2. Here, there is no chance for other singularities to be "caught" between the two contours and the entire field arises as the body wave contribution due to the saddle point. (Note that this is the case of a vertical—possible multiply reflected—ray trajectory.) As above, however, singularities to the right of $\Gamma = S$ may yet appear close enough to S' to influence the value of the integral over S'.

In summary, our approach may be viewed as an attempt to replace the contour Γ' by the contour S'. When there are no singularities in the primary τ-domain–equivalently, no singularities in the primary p-domain–the replacement is justified by Cauchy's theorem; when there are singularities in the primary τ-domain, we must account for these singularities in the contour deformation and S' is only the tail of (one of the) loop contours in the τ-domain.

This approach to the Cagniard-de Hoop method is reminiscent of van der Waerden's (1951) approach to the method of steepest descents, which starts exactly the same way. Indeed, after the deformation of contour in the τ-domain, the user has the choice of (i) applying asymptotic analysis to the resulting "loop" integral(s) [Watson's lemma] (Bleistein, 1984) or (ii) continuing to obtain the exact, although usually implicit, time domain solution by completing the Cagniard-de Hoop analysis. In

the former case, one obtains the large s expansion, from which a progressing wave expansion in the time domain can be derived.

In some sense, we have come full circle back to Cagniard's (1939, 1962) approach, using two complex planes. In that work the author described the mapping from p to τ in much more detail than we think is necessary. Indeed, de Hoop (1958) points out that one of his motivations for his modification of the Cagniard method was the difficulties of coping with the complex mapping. Furthermore, the important role that we see for the path of steepest ascent was not a part of that original method. We believe that our "equal status" point of view extracts the best of both methods.

In the next section, we discuss the transformation from Fourier transforms in traditional wave number k (one transverse dimension) or wave vector $\boldsymbol{k}$ and frequency ω to slowness p or slowness vector $\boldsymbol{p}$ and Laplace transform variable s. We do this for two reasons. First, for some users deriving a solution representation in the former pair of variables is more natural. Second, in the former variables we can treat a traditional noncausal problem—the Sommerfeld problem with acute angle of incidence of the plane wave—that is not amenable to analysis in the Laplace domain. In the third section, we discuss the transformation from p to τ with emphasis on features that we believe are important to our approach to the method. Finally, we apply our approach to some standard examples of the Cagniard method and then to the nonstandard Sommerfeld example.

TRANSFORMATION OF FOURIER INTEGRALS

In our analysis of waves in layered media we start from a Fourier transform in time, rather than from the Laplace transform typical of the literature of the Cagniard-de Hoop method. We think this is a useful choice because Fourier representations for solutions of wave propagation problems are far more common than Laplace represen-

tations in the modern literature with the Cagnaird-de Hoop method being almost the sole exception to this trend.

For "causal" problems, the Fourier representation, just as the Laplace representation, is a transform on a semi-infinite domain from some finite time to infinity. Most problems of interest start from some finite time. Indeed, even some problems described in terms of a plane wave incident from infinity can be reformulated as causal problems. We will discuss this point further below in connection with the Sommerfeld half-plane problem. Thus, for a function $V(x,z,t)$, we define in the causal case

$$v(x,z,\omega) = \int_{t_0}^{\infty} V(x,z,t)\exp\{i\omega t\}\,dt. \tag{0.4}$$

It follows that the temporal Fourier transform is an analytic function of ω in some upper half ω-plane, usually not including the real axis where singularities of the transform reside. Of course, this upper half-plane is exactly the right half-plane of analyticity of the Laplace transform. The value of the solution representations for real values of ω are obtained by analytic continuation from this upper half-plane. In fact, we can and will consider only the upper *right half-plane* $\mathrm{Re}\,\omega \geq 0$, and determine the solution elsewhere by analytic continuation. With this convention, the specific branches of multi-valued functions of ω and the spatial transform variable(s) are uniquely defined, as is the avoidance of these singularities on the contour(s) of integration of the inverse transform.

In most cases of interest in wave propagation problems, the lower boundary of the half-plane of analyticity is the Re ω axis. We assume that is the case here, although it is not crucial to the analysis below. However, it does allow us to define the quarter plane of our attention by the condition

$$\omega = |\omega|\exp\{i\alpha\},\ 0 < \alpha = \arg\omega \leq \pi/2. \tag{0.5}$$

For problems in two spatial dimensions, the Fourier (k,ω) representation to be studied takes the form

$$\begin{aligned} v(x,z,\omega) &= \int_{-\infty}^{\infty} g(k,\omega)\exp\{i\varphi(k,\omega,x,z)\}\,dk, \\ \varphi(k,\omega,x,z) &= kx + \sum_{j=1}^{J} h_j\sqrt{(\omega/c_j)^2 - k^2}. \end{aligned} \tag{0.6}$$

The function g is assumed to have the structure

$$g(k,\omega) = (\omega)^n\, g(k/\omega, 1). \tag{0.7}$$

This is the form of g for a point source; for more complex sources, the solution is obtained by convolution with the solutions of the type presented here.

With our assumption that $\operatorname{Im}\omega > 0$, there are no singularities of φ (or g) on the $\operatorname{Re} k$-axis, the path of integration in (0.6). In particular, the branch points at ω/c_j lie in the first quadrant (or positive imaginary axis) of the k-plane, and the branch points at $-\omega/c_j$ lie in the third quadrant (or negative imaginary axis), because we have fixed $\operatorname{Re}\omega \geq 0$.

Let us introduce the change of variable of integration

$$k = \omega p, \tag{0.8}$$

and consider the image of the integration contour in the p-plane and the location of singularities of the integrand there, as well.

First, note that for k real and $\arg\omega = \alpha$ (0.5), on the path of integration

$$\arg p = -\alpha. \tag{0.9}$$

This means that as $\arg\omega$ increases from zero to $\pi/2$ the contours of integration are a family of straight lines through the origin, passing from the first quadrant to the third.

To achieve the form (0.1), it is necessary to pick $\alpha = \pi/2$. While in principle one could attempt an analog to the Cagniard-de Hoop theory with other choices of α, this choice is optimal as we will show later. In this case, the contour of integration is the imaginary axis starting at $+i\infty$ and ending at $-i\infty$. Later, we will reverse this direction by multiplying the integrand by -1.

Before proceeding any further with this line of analysis, let us examine the singularities of the integrand. In particular, note from (0.6) that

$$\varphi(k,\omega,x,z) = \omega\left[px + \sum_{j=1}^{J} h_j\sqrt{(1/c_j)^2 - p^2}\right]. \tag{0.10}$$

Thus, the integrand in p has branch points at $\pm 1/c_j$, $j = 1,\ldots,J$, and, as α increases from zero to $\pi/2$, the contour simply rotates away from these branch points.

On the other hand, suppose that $g(k,\omega)$ had singularities in the second or fourth quadrant. Then we would have to take account of the effect of passing the contour of integration "through" these singularities. For poles, that would simply amount to including a residue as part of the transformation process; for branch points, a loop integral enclosing the branch point would have to be included in the analysis. Such singularities arise only in noncausal problems—an example of this type is included in a later section.

Choosing $\alpha = \pi/2$ amounts to evaluating the Fourier transform for a purely imaginary value of the transform variable ω. Alternatively, we can set

$$\omega = is \tag{0.11}$$

with s real and positive when $\alpha = \arg\omega = \pi/2$.

What we have just done is change a Fourier transform into a Laplace transform. However, we have done it with enough care to alert the reader to the possibility of contributions from singularities of the integrand of a type we will see below in

a noncausal example. We note that converting the forward Fourier transform to a forward Laplace transform implies that the inverse transform now takes the form of the usual inverse Laplace transform.

We proceed below with our analysis for s real and positive. All results can be extended to complex s by analytic continuation techniques; however, this is not necessary for the Cagniard-de Hoop method since the explicit inversion integration is not performed.

We have one other small trick to offer. We use the transformation (0.8) for x positive and we use $k = -\omega p$ for x negative. That is, we use $k = \omega p \,\mathrm{sgn}(x)$. This reverses the orientation of the contour, but introduces a compensating minus sign in dk/dp. These are nullifying effects.

Furthermore, functions of k^2, such as the square roots appearing in φ are unaffected by this trick, while the expression kx is transformed into $\omega p|x|$. This will prove useful below. The amplitude g need not be a function of k^2 and some care is required in dealing with this function.

In summary, taking account of this additional trick and the contour rotation, as well as the change of variables from ω to s, we set

$$k = isp\,\mathrm{sgn}(x). \tag{0.12}$$

For this function $dw/dp > 0$ at $p = 0$ for x nonzero. Since it is our intention to make $\tau = w$ the new variable of integration, this will insure that the image Γ of the $\mathrm{Re}\, p$ axis, the contour of integration in (0.1), has an orientation that is independent of $\mathrm{sgn}(x)$. This was the motivation for using a change of variables that depends on $\mathrm{sgn}(x)$.

Under this combined change of variables and rotation Γ, the contour of integration in (0.1) is the imaginary axis oriented from $-i\infty$ to $i\infty$ and

$$f(p) = -g(p\,\mathrm{sgn}(x), 1) \;=\; -(is)^{-n} g(isp\,\mathrm{sgn}(x), is),$$

$$u(r, z, s) \;=\; v(x, z, is)(is)^{-n-1}. \tag{0.13}$$

Here we have allowed for u to be the true transformed field within a power of is. In general, we neglect multiplication by powers of s here, since they can be dealt with back in the space/time domain. Integer powers of s are equivalent to differentiation or integration in the time domain; noninteger powers of s correspond to fractional derivatives or integrals in the time domain, which are equivalent to convolution with fractional powers of t. The extra minus sign in the transformation from g to f arises from the fact that the image of the integration path in (0.6) is the imaginary axis oriented *downward*, whereas Γ in (0.1) is oriented *upward*. Had we not assumed the form of g in (0.7), then we would not have ended up with f being a function of p alone in this equation. Authors starting from Laplace transforms assume this form of f to begin their analysis.

For three-dimensional problems, we start from a representation of the form

$$v(x, y, z, \omega) = \int_{-\infty}^{\infty} g(k_1, k_2, \omega) \exp\{i\varphi(k_1, k_2, \omega, x, y, z)\}\, dk_1\, dk_2,$$

$$\varphi(k_1, k_2, \omega, x, y, z) = k_1 x + k_2 y + \sum_{j=1}^{J} h_j \sqrt{(\omega/c_j)^2 - k_1^2 - k_2^2}. \tag{0.14}$$

Again, we assume that g has the special form

$$g(k_1, k_2, \omega) = (\omega)^n\, g(k_1/\omega, k_2/\omega, 1). \tag{0.15}$$

To transform this integral, we first introduce the polar coordinates (r, ϕ),

$$x = r\cos\phi,\;\; y = r\sin\phi. \tag{0.16}$$

Next, we apply the de Hoop transformation (de Hoop, 1960) in the k-domain,

$$k_1 = \kappa_1 \cos\phi - \kappa_2 \sin\phi,$$

$$k_2 = \kappa_1 \sin\phi + \kappa_2 \cos\phi; \tag{0.17}$$

and we note that

$$k_1 x + k_2 y = \kappa_1 r. \tag{0.18}$$

In these new variables, (0.14) becomes

$$v(x,y,z,\omega) = \int_{-\infty}^{\infty} \tilde{g}(\kappa_1,\kappa_2,\omega) \exp\{i\tilde{\varphi}(\kappa_1,\kappa_2,\omega,x,y,z)\}\, d\kappa_1\, d\kappa_2,$$

$$\begin{aligned} \tilde{w}_1(\kappa_1,\kappa_2,i\omega,x,y,z) &= \kappa_1 r + \sum_{j=1}^{J} h_j \sqrt{(\omega/c_j)^2 - \kappa_1^2 - \kappa_2^2}, \\ \tilde{g}(\kappa_1,\kappa_2,\omega) &= g(k_1,k_2,\omega). \end{aligned} \tag{0.19}$$

The function $\tilde{g}$ retains the property (0.15). We proceed with the same scaling as above, except that now we must scale both κ_1 and κ_2. The rotation in ω rotates both transformed integrals. The same caveats above must be observed here regarding passing through singularities.

In summary,

$$\kappa_1 = isp,\ \kappa_2 = sq,\ \omega = is, \tag{0.20}$$

leads to the representation of the form of (0.1), except that now both f and w depend on q:

$$f(p) = -\tilde{g}(p,-iq,1) = -(is)^{-n}\tilde{g}(isp,sq,is),$$

$$u(r,z,s) = (is)^{-n-1}s^{-1}v(x,y,z,is). \tag{0.21}$$

For the purposes of the Cagniard-de Hoop method, we treat q as a parameter whose presence need not be specifically noted in the arguments of these functions. However, it should be noted that q changes the meaning of the slowness value $1/p_j$, in that

$$\begin{aligned} p_j &= 1/c_j, \qquad \text{two dimensions,} \\ p_j &= \sqrt{1/c_j^2 + q^2}, \qquad \text{three dimensions.} \end{aligned} \tag{0.22}$$

Furthermore, after applying the Cagniard method to determine $U(r,z,t)$, it is necessary to integrate the result with respect to q over $(-\infty,\infty)$.

In summary, we have shown how Fourier representations of both two- and three-dimensional wavefields in stratified media can be reduced to the same integral form, Equation (0.1).

ANALYSIS OF THE EXPONENT

Here we consider the complex change of variables

$$\tau = w(p,r,z) = pr + \sum_{j=1}^{J} h_j \sqrt{p_j^2 - p^2}, \tag{0.23}$$

from p to τ. Under this change of variables, the integral in (0.1) becomes

$$u(x,z,s) = \int_{\Gamma'} f(p(\tau)) \frac{dp}{d\tau} e^{-s\tau}\, d\tau. \tag{0.24}$$

We need to know the image Γ' in the τ-plane of the contour of integration in (0.1). That original contour Γ is just the imaginary axis. Because we want to deform this image contour onto the $\mathrm{Re}\,\tau$ axis, we also need to understand the conformal mapping of the image region between Γ' and the $\mathrm{Re}\,\tau$ axis. In this manner, we will identify those singularities that must be crossed in deforming one contour into the other.

The Image of Γ

We consider now the image of the contour Γ under the mapping (0.23). For this image, let us set

$$p = i\sigma, \ -\infty < \sigma < \infty. \tag{0.25}$$

With this choice,

$$\mathrm{Re}\,\tau = \sum_{j=1}^{J} h_j \sqrt{p_j^2 + \sigma^2}, \quad \mathrm{Im}\,\tau = \sigma r, \tag{0.26}$$

so that $\mathrm{Re}\,\tau$ is even and $\mathrm{Im}\,\tau$ is odd on the image contour Γ'. Note also that

$$\frac{d\tau}{dp} = r - \sum_{j=1}^{J} \frac{h_j p}{\sqrt{p_j^2 - p^2}}. \tag{0.27}$$

In particular,

$$\left.\frac{d\tau}{dp}\right|_{p=0} = r > 0. \tag{0.28}$$

From this it follows that $\arg d\tau = \pi/2$, because $\arg dp = \pi/2$ at $p = 0$. Thus, the contour is directed vertically upward at the image point

$$\tau(0) = \sum_{j=1}^{J} h_j p_j, \tag{0.29}$$

which is the travel time along a vertical raypath from the source depth to the observation depth. That path includes all multiple reflections at interfaces that are implied by the terms of the sum in $w(p, r, z)$.

In general, on this image path

$$\mathrm{Re}\,\tau \to |\sigma| \sum_{j=1}^{J} h_j, \quad \mathrm{Im}\,\tau \to \sigma r, \ |\sigma| \to \infty, \tag{0.30}$$

and

$$\frac{\mathrm{Im}\,\tau}{\mathrm{Re}\,\tau}\mathrm{sgn}(\sigma) \to \frac{r}{\sum_{j=1}^{J} h_j}, \ |\sigma| \to \infty. \tag{0.31}$$

That is, the image contour has an asymptote in the τ-plane with slope proportional to the ratio of the horizontal travel distance to the vertical offset. In the simplest

case, $J = 1$, this curve is one branch of a hyperbola. For larger values of J, the basic hyperbola-like nature of a symmetric curve with symmetric asymptotes still holds. Figure 0.2 is an example of an image contour Γ' for a case in which $J = 2$ and the two propagation speeds are 3km/sec and 4km/s with $h_1 = h_2 = 1.2$km and $r = 2.5$km.

Because the classic Cagniard integration path in the complex p-plane is also hyperbolic-like, the reader is cautioned not to confuse it with the previously discussed image contour Γ' of the imaginary p-axis. This path is in the τ-domain; the Cagniard path is in the p-domain.

The Saddle Points of w

Saddle points are defined as those points at which $dw/dp = d\tau/dp = 0$. From (0.27), one can verify that there is always a point on the $\mathrm{Re}\, p$ axis where this is true. In that equation, one can see that

$$\frac{d\tau}{dp} \to -\infty, \text{ as } p \to \min_j(p_j). \tag{0.32}$$

Because $d\tau/dp$ is positive at $p = 0$, from (0.28), $d\tau/dp$ must pass through zero somewhere on this interval. This is the saddle points to be denoted by p_s. At this point,

$$r = \sum_{j=1}^{J} h_j \frac{p_s}{\sqrt{p_j^2 - p_s^2}}. \tag{0.33}$$

This equation defines the geometrical optics ray that connects the origin with the point (x, z) including multiple reflections and refractions satisfying Snell's law. To see this latter point, observe that Snell's law for reflection and refraction guarantees that

$$p_s = p_j \sin\theta_j, \quad j = 1, J, \tag{0.34}$$

is the same for each j (even for mode converted waves). Equation (0.32) assures that $p_s < \min_j(p_j)$; and thus, that each θ_j is real. The horizontal travel in the jth layer is

given by $h_j \tan\theta_j$; thus, the total horizontal travel is

$$r = \sum_{j=1}^{J} h_j \tan\theta_j. \tag{0.35}$$

If we use (0.34) to define $\tan\theta_j$ in terms of p_s and p_j, the result is (0.33).

The saddle point p_s is a significant point for our analysis. At this point, the mapping from p to τ ceases to be conformal; that is, the angle between two intersecting arcs in the p-domain will not be preserved in the τ-domain. To determine how this angle is changed, it is necessary to find the first nonvanishing derivative at p_s. To this end, we differentiate (0.27) to obtain

$$\frac{d^2\tau}{dp^2} = -\sum_{j=1}^{J} \frac{h_j p_j^2}{\left[p_j^2 - p^2\right]^{3/2}}. \tag{0.36}$$

The explicit formula shows that $d^2\tau/dp^2$ is negative on the interval from 0 to $\min_j(p_j)$. This establishes that $p = p_s$ is the *only* saddle point on this interval and that the second derivative is negative at this saddle point. Let us set

$$\tau(p_s) = \tau_s. \tag{0.37}$$

Because $d^2\tau/dp^2$ is nonzero,

$$\tau - \tau_s \approx \frac{1}{2}\frac{d^2\tau(p_s)}{dp^2}(p - p_s)^2, \tag{0.38}$$

from which it follows that changes in argument of $p - p_s$ are *doubled* in the τ-domain.

Of particular interest to us are the paths through p_s on which $\operatorname{Im} w =$ constant. In our case, that constant is zero, since $w(p_s)$ is real. Of necessity, the image of these paths must be a segment of the $\operatorname{Re}\tau$ axis, and these paths $\operatorname{Im} w = 0$ through the saddle point are segments of the Cagniard path.

In the method of steepest descents, these paths of constant $\operatorname{Im} w$ are called paths of steepest ascent or descent. The reason is that when we think in terms of the surface

Re w, these are the paths of maximal change in Re w away from the reference point, or literally the directions of steepest ascent and descent on this surface. In the method of steepest descents, the paths of steepest *descent* are the paths of interest (since the exponent of interest is $+sw$); here, the paths of choice are the paths of steepest *ascent* (since the exponent of interest is $-sw$) because in either case we are interested in the paths on which the integrand decays exponentially to zero at a maximal rate. We will denote by S the contour made up of the two paths of steepest ascent through p_s oriented in the direction of ascent in the upper half-plane. Figure 0.2 shows S' for the same example considered in Figure 0.1. Note that Figure 0.2 shows a contour in the τ-domain, while Figure 0.1 shows a contour in the p-domain. The contour Γ' in Figure 0.2 is the image of the Im p axis. As noted above, the image S' of the contour S in Figure 0.1 is the doubly covered Re τ axis, starting at τ_s and extending to infinity. This will be verified below. When viewed as a conformal mapping, the image of the region between the Γ and S in the p-domain (Figure 0.1) is the region between Γ' and S' in the τ-domain (Figure 0.2). As noted in the introduction, we refer to this former region of the p-plane as the *primary p-domain* and we refer to its image in the τ-domain as the *primary τ-domain.*

On S, Im $w = 0$, as required; however, there are two curves through p_s with this property and they are orthogonal to one another. How can we see that the image of the contour indicated here is S', as claimed? Note first, from (0.36) and (0.38) that

$$\tau_s - \tau \approx A(p_s - p)^2 \tag{0.39}$$

with $A > 0$. Here, reversing the order of $\tau's$ on the left side of the equation has allowed us to express the approximation (0.38) in terms of a positive constant, A. Reversing the order of the $p's$ on the right side of the equation allows us to express the right side in terms of an expression for which we know the argument at $p = 0$ and then, by continuity allows us to know the argument everywhere. In particular, one

can verify that when p moves from the origin to a point on S above p_s and nearby, $\arg(p_s - p) \approx -\pi/2$ and $\arg(\tau_s - \tau) \approx -\pi$. Similarly, when p moves from the origin to a point on S below p_s and nearby, $\arg(p_s - p) \approx +\pi/2$ and $\arg(\tau_s - \tau) \approx +\pi$. In either case, $\tau_s - \tau$ is negative as required. One can further verify that on the alternative paths of constant $\operatorname{Im} w$, $\operatorname{Re} w$ decreases. That is, the image of these paths is the $\operatorname{Re}\tau$ axis to the left of τ_s.

Of special interest is the $\operatorname{Re} p$ axis to the right of p_s. Here we must have $\arg(p_s - p) = \pm\pi$, depending upon whether this region was reached by p passing above $(-)$ or below $(+)$ p_s when starting from $p = 0$. It follows from (0.39) that for these cases $\arg(\tau_s - \tau) = \pm 2\pi$, which are choices of the argument outside of the primary τ-domain. These values of τ correspond to points on the second Riemann sheet of the mapping from p to τ and values, $\tau < \tau_s$.

It will prove useful to evaluate τ_s. To this end, we use (0.33) in (0.23) to find

$$\begin{aligned} \tau_s &= \sum_{j=1}^{J} h_j \frac{p_s^2}{\sqrt{p_j^2 - p_s^2}} + h_j \sqrt{p_j^2 - p^2} \\ &= \sum_{j=1}^{J} h_j \frac{p_j^2}{\sqrt{p_j^2 - p_s^2}}. \end{aligned} \tag{0.40}$$

Let us define

$$r_j = \frac{h_j p_s}{\sqrt{p_j^2 - p_s^2}}, \quad \rho_j = \sqrt{r_j^2 + h_j^2}. \tag{0.41}$$

That is, r_j is the segment of the offset r at $p = p_s$ in the j-th layer and ρ_j is the length of the ray segment in the j-th layer. Substitution of the definition of r_j into the definition of ρ_j yields

$$\rho_j = \frac{h_j p_j}{\sqrt{p_j^2 - p_s^2}}, \tag{0.42}$$

and

$$\tau_s = \sum_{j=1}^{J} \rho_j p_j \tag{0.43}$$

is the total traveltime along the ray. When we compare this result with (0.29), we see that

$$\tau_s \geq \tau(0), \tag{0.44}$$

with equality holding only for $r = 0$. Indeed, from (0.36), τ_s is the *maximum* of τ for $0 < p < \min_j(p_j)$ and this inequality holds for $\tau(0)$, replaced by $\tau(p)$ for any p in this interval.

The point τ_s is a branch point of the integrand in (0.3). To see why this is so, let us solve (0.38) for p:

$$p - p_s \approx \sqrt{\frac{2(\tau - \tau_s)}{d^2\tau_s/dp^2}}. \tag{0.45}$$

Differentiation of this equation yields

$$\frac{dp}{d\tau} \approx \frac{1}{\sqrt{2(\tau - \tau_s)d^2\tau_s/dp^2}}, \tag{0.46}$$

which verifies the claim.

We can draw an important conclusion from this observation. The image in the τ-domain of the steepest descent path in the p-domain is a segment of the $\mathrm{Re}\,\tau$ axis that lies to the right of the image of the imaginary axis as shown in Figure 0.2.

In the τ-domain, we are most concerned with the region in which $0 \leq \arg(\tau - \tau_s) < 2\pi$ that lies in the primary τ-domain. To see this, note from (0.36) that $d^2\tau/dp^2 < 0$ and, of necessity, $\arg p - p_s = \pi/2,\ 3\pi/2$, for $\tau - \tau_s$ to be positive. When we take $\arg d^2\tau/dp^2 = -\pi$, we find that these two directions correspond to $\arg \tau - \tau_s = 0,\ 2\pi$, respectively. Then, in this neighborhood, values of $\arg p - p_s$ less than $\pi/2$ or greater than $3\pi/2$ must correspond to images points with $\arg \tau - \tau_s$ less than zero or greater than 2π, respectively. These regions correspond to another *Riemann sheet* of the multi-sheeted surface of the τ-domain.

Of particular importance, singular points of $f(p)$ in the primary p-domain map into points in the primary τ-domain. As previously noted, not all of these need to

be singular points of the integrand $f(\tau)dp/d\tau$ in (0.3). For those that are singular points after transformation, deformation of the contour Γ' onto the $\mathrm{Re}\,\tau$ axis cannot proceed without including loop contours around these points. On the other hand, singularities to the *right* of the path of steepest descent in the p-domain and out of the primary p-domain, must of necessity map onto these *other sheets* of the Riemann surface.

The Branch Points of w

We turn now to consideration of the points p_j which are the branch points of $w(p)$ in (0.2). In the neighborhood of p_j,

$$\tau - \tau(p_j) \approx h_j\sqrt{2p_j}\sqrt{p_j - p} + O(p_j - p), \tag{0.47}$$

from which it follows that

$$p_j - p \approx \frac{(\tau - \tau(p_j))^2}{2p_j h_j^2} + O((\tau - \tau(p_j))^3). \tag{0.48}$$

From the first equation here, we conclude that $\sqrt{p_j - p}$ is *linear* in $\tau - \tau(p_j)$. Thus, if this square root appears in $f(p)$, it is *not* a branch point of $f(p(\tau))$. From the second equation here, we conclude that $dp/d\tau$ is also *linear* in $\tau - \tau(p_j)$. Thus, the branch points of $w(p)$ are not *a priori* branch points of the transformed integrand $f(p(\tau))dp/d\tau$ of (0.3).

On the other hand, other singular points of $f(p)$ must of necessity be singularities of corresponding type—branch point, pole, etc.—of $f(p(\tau))$, because $d\tau/dp$ is finite and nonzero at such points.

The Choice $\alpha = \pi/2$.

We close this section by returning to the question of the choice of final argument $\pi/2$ for ω. For any other choice, the path Γ would not be vertical. Then, for r near

enough to zero, Γ would intersect S, in which case the image domain in τ becomes much more complicated. In particular, the image path Γ' would cut through the image path S' and part of the primary τ-domain would be on the second Riemann sheet.

On the other hand, it has been shown that knowing the Laplace transform for real values of s suffices for the determination of its inverse function (technically, up to a function of measure zero, but uniquely at points where the inverse transform is at least left- or right-continuous). This follows from the observation that the Laplace transform must be analytic in some right-half $s-$plane and Lerch's theorem [Sneddon, 1972, Widder, 1959], which assures uniqueness of the Laplace inversion of such functions. Then, one need only observe that an analytic function is determined in its domain of analyticity by its values on a line segment in that domain, no matter how small. Any segment of the Re s axis will do. It is standard in the literature to simply state that knowledge of the Laplace transform on the real axis suffices to determine the inverse function (in the time domain) uniquely.

EXAMPLES

Here we will demonstrate the application of the Cagniard-de Hoop method on various examples designed to demonstrate the analysis above and bring out the features of this interplay of two complex planes. The reader should note that the image of the steepest ascent path in the p-domain is always at least a part of the loop integral path around the real axis in the τ-domain and, sometimes, may be all of it. Whether or not it is all of that path depends on whether or not there are other singularities of $f(p)$ in the primary p-domain other than branch points of order one-half at the same locations at the branch points of the exponent $w(p, r, z)$.

Two-dimensional free space Green's function

In this first example, the only singularity of the integrand in the τ-domain will be the branch point at τ_s. We will verify further that the integrand is analytic at the image of the (single) branch point of $w(r, z, p)$.

We consider

$$v(x, z, \omega) = -\frac{1}{4\pi i}\int_{-\infty}^{\infty} \frac{dk}{\sqrt{\omega^2/c_1^2 - k^2}} \exp\left\{i[kx + \sqrt{\omega^2/c_1^2 - k^2}|z|]\right\}. \tag{0.49}$$

This is an integral representation of the two-dimensional Green's function for the Helmholtz equation for acoustic waves in a constant density medium,

$$\nabla^2 u + \frac{\omega^2}{c_1^2} u = -\delta(x)\delta(z). \tag{0.50}$$

Here ∇^2 is the two dimensional Laplacian. See Bleistein (1984), for example.

This representation is a special case of (0.6) and the transformation of the solution proceeds as in the discussion below (6) to yield (0.1) with w defined by (0.2) and $J = 1$. That is,

$$u(x, z, s) = \frac{1}{4\pi i}\int_\Gamma -\frac{dp}{\sqrt{p_1^2 - p^2}} \exp\{-sw(p, |x|, z)\} \tag{0.51}$$

with w given by

$$w(p, |x|, z) = p|x| + \sqrt{p_1^2 - p^2}|z|, \; p_1 = 1/c_1. \tag{0.52}$$

In this example, the only critical points of the integrand are the branch points at $\pm p_1$ and the saddle point determined by (0.33) with $r = |x|$:

$$p_s = p_1|\sin\theta|, \quad x = \rho\sin\theta, \quad z = \rho\cos\theta, \; \rho = \sqrt{x^2 + z^2}. \tag{0.53}$$

We need no index on θ here because there is only one value, p_1.

The transformation (0.23) in this case is

$$\tau = w(p, |x|, z) = p|x| + \sqrt{p_1^2 - p^2}|z| \tag{0.54}$$

and (0.24) becomes

$$u(x,z,s) = \frac{1}{4\pi i}\int_{\Gamma'} \frac{dp}{d\tau}\frac{d\tau}{\sqrt{p_1^2 - p^2}} \exp\{-s\tau\}, \tag{0.55}$$

with Γ' as shown in Figure 0.2 except that the specific numbers of that example are not relevant here. The theory assures us that the integrand has no singularities except for the branch point at

$$\tau_s = p_1\rho, \tag{0.56}$$

and that there are no other singularities of the integrand in (0.24). We will explicitly verify that below.

We can now close the contour of integration Γ' around the branch point at τ_s to obtain a loop integral on the contour S' as shown in Figure 0.1. We denote the solution $p(\tau)$ for τ on the upper side of the loop by p_+ and the solution $p(\tau)$ for τ on the lower side of the loop by p_-. Then we can write

$$u(x,z,s) = \frac{1}{4\pi i}\int_{\tau_s}^{\infty} \left[\frac{dp_+}{d\tau}\frac{1}{\sqrt{p_1^2 - p_+^2}} - \frac{dp_-}{d\tau}\frac{1}{\sqrt{p_1^2 - p_-^2}}\right] \exp\{-s\tau\}d\tau. \tag{0.57}$$

Now the time-domain solution can be read off as the integrand here. However, there is one further simplification that comes from the fact that the two terms in the integrand are *complex conjugates* of each other. This fact observation follows from the *Schwarz reflection principle* [Levinson and Redheffer, 1970], which assures us that an analytic function must assume complex conjugate values across a line in its domain of analyticity on which the function is real. Here the line along which the function $p(\tau)$ is real, is the line $p_1|z| < \tau < \tau_s = p_1\rho$, which is the image of $0 < p < p_s$ where we know that w is real. Thus, complex conjugate points in either domain correspond to complex conjugate points in the other and we conclude that

$$U(x,z,t) = \mathrm{Im}\left\{\frac{dp_+}{d\tau}\frac{1}{2\pi\sqrt{p_1^2 - p_+^2}}\right\} H(t - \tau_s). \tag{0.58}$$

In this equation, $H(t)$ is the *Heaviside function*, equal to unity for positive argument and zero for negative argument.

For this particular case, we can explicitly solve for $p(\tau)$ because (0.54) is equivalent to a quadratic equation. The solution is

$$p = \left[|x|\tau - |z|\sqrt{p_1^2\rho^2 - \tau^2}\right]/\rho^2. \tag{0.59}$$

In this solution, it was necessary to make a choice of sign of the square root. We chose the sign for which

$$p = 0 \iff \tau = p_1|z|,$$

which is consistent with (0.54). The other choice of sign of the square root corresponds to the mapping of p to the *second Riemann sheet* of the τ-domain. We see here that the only singularities of this function are at $\tau = \pm p_1\rho = \pm\tau_s$. One of these is as predicted by the theory and the other is completely outside the domain of interest, since it is not in the primary τ-domain.

One can further confirm that

$$\sqrt{p_1^2 - p^2} = \left[|z|\tau + |x|\sqrt{p_1^2\rho^2 - \tau^2}\right]/\rho^2, \tag{0.60}$$

which also is singular only at $\pm\tau_s$ and *not* at $\tau(p_1) = p_1|x|$. This is as predicted by the theory.

Finally,

$$\frac{dp}{d\tau} = \frac{|z|\tau + |x|\sqrt{p_1^2\rho^2 - \tau^2}}{\rho^2\sqrt{p_1^2\rho^2 - \tau^2}}. \tag{0.61}$$

Since the Heaviside function in (0.58) confines the nonzero portion of the solution to $t > \tau_s = p_1\rho$, and since we wrote this result in terms of p_+, we must determine what happens to the square root in (0.59) when we pass *over* the branch point at $p_1\rho$ in the τ-domain. What is crucial here is that $\arg(p_1\rho - \tau)$ varies from 0 to $-\pi$

on this trajectory. We conclude then that the square root must have an argument of $-\pi/2$ (essentially, a multiplier of $-i$ on a real positive square root). That is,

$$p_+ = \left[|x|\tau + i|z|\sqrt{\tau^2 - p_1^2\rho^2}\right]/\rho^2, \ \tau \geq p_1\rho. \tag{0.62}$$

However, we need not deal separately with the derivative and $f(p_+(\tau))$ because it follows from (0.60) and (0.61) that

$$\frac{dp_+}{d\tau}\frac{1}{\sqrt{p_1^2 - p_+^2}} = \frac{i}{\sqrt{\tau^2 - p_1^2\rho^2}}, \ \tau > p_1\rho. \tag{0.63}$$

Now we can evaluate (0.58) explicitly to obtain

$$U(x,z,t) = \frac{H(t-\rho/c_1)}{2\pi\sqrt{t^2 - \rho^2/c_1^2}}. \tag{0.64}$$

Here we return to the use of the propagation speed c_1, rather than the slowness p_1. This is the two-dimensional free space Green's function for the wave equation (0.50).

Point Source over a Half Space

As a second example we consider

$$v(x,z,\omega) = -\frac{1}{4\pi i}\int_{-\infty}^{\infty}\frac{dk}{\sqrt{\omega^2/c_1^2 - k^2}}R(k/\omega)\exp\{i[kx + \sqrt{\omega^2/c_1^2 - k^2}(2h - z)]\}, \tag{0.65}$$

with

$$R(k/\omega) = \frac{\sqrt{1/c_1^2 - k^2/\omega^2} - \sqrt{1/c_2^2 - k^2/\omega^2}}{\sqrt{1/c_1^2 - k^2/\omega^2} + \sqrt{1/c_2^2 - k^2/\omega^2}}. \tag{0.66}$$

This is the upward scattered acoustic wave in a constant density medium for a point source at height h, over a half space. See Bleistein (1984), for example. This solution, when added to the previous one, provides the total response above the interface between two homogeneous half spaces with different acoustic speeds.

This solution again fits the form of (0.6) and the transformation of the solution proceeds as in the discussion below that equation to yield (0.1) with w defined by

(0.2) and $J = 1$. That is,

$$u(x,z,s) = \frac{1}{4\pi i}\int_\Gamma \frac{dp}{\sqrt{p_1^2 - p^2}} R(p)\exp\{-sw(p,|x|,z)\}, \tag{0.67}$$

with

$$\begin{aligned} w(p,|x|,z) &= p|x| + \sqrt{p_1^2 - p^2}(2h - z), \\ R(p) &= \frac{\sqrt{p_1^2 - p^2} - \sqrt{p_2^2 - p^2}}{\sqrt{p_1^2 - p^2} + \sqrt{p_2^2 - p^2}}, \\ p_1 &= 1/c_1,\ p_2 = 1/c_2. \end{aligned} \tag{0.68}$$

The new feature of this example is that $f(p)$ now has a branch point at p_2, which is *not* a branch point of the exponent w. As in the previous example, the branch point at p_1 appears to the same order in $f(p)$ and $w(p,|x|,z)$.

Note that, except for replacing $|z|$ by $2h - z$, the analysis of the transformation from p to τ is exactly as in the previous example. In particular, the saddle point determined by (0.33) with $r = |x|$ becomes

$$p_s = p_1|\sin\theta|, \quad x = \rho\sin\theta, \quad 2h - z = \rho\cos\theta, \ \rho = \sqrt{x^2 + (2h - z)^2}. \tag{0.69}$$

The region in which $2h - z > 0$ corresponds to $|\theta| < \pi/2$.

The transformed integral (0.24) for this case is

$$u(x,z,s) = \frac{1}{4\pi i}\int_{\Gamma'} \frac{d\tau}{\sqrt{p_1^2 - p^2}} R(p(\tau))\frac{dp}{d\tau}\exp\{-s\tau\}, \tag{0.70}$$

with Γ' as shown in Figure 0.2, except that again, the specific numbers of the figure are not relevant here.

We must be concerned with the location of the branch point p_2 and its image in the τ-domain. In particular, we must know when the image falls in the primary τ-domain. If $p_2 > p_1$, this cannot happen, since $p_s < p_1 = \min(p_1, p_2)$; see preceding

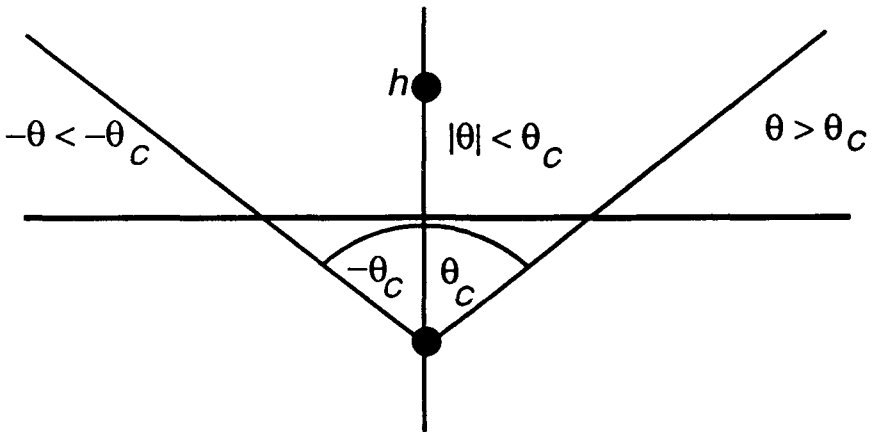

FIG. 0.3. Physical domain showing pre- and post-critical regions defined in terms of θ.

discussion on the location of the saddle point. Therefore, the interesting case occurs when

$$p_2 < p_1 \text{ or } c_1 < c_2. \tag{0.71}$$

Of course, the reader familiar with this problem will observe that this is, indeed, the case in which *head waves* arise and that they manifest themselves in the solution through the effect of this second branch point. We proceed with this more interesting case.

We introduce the *critical angle*, θ_c by the equation

$$p_2 = p_1 \sin\theta_c \tag{0.72}$$

and note that p_2 will be in the primary p-domain if

$$\sin\theta_c < |\sin\theta|. \tag{0.73}$$

From Figure 0.3, we can see that this is the *post-critical* reflection region in which the incident wave is totally reflected. Therefore, for this physical region we now know

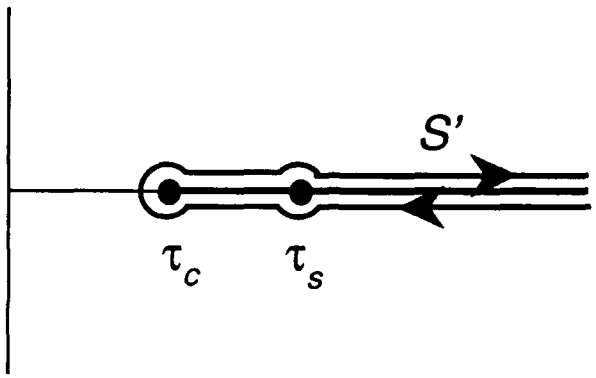

FIG. 0.4. Deformed path of integration in the τ-domain for p_2 in the primary p-domain.

that the image point τ_c, given by

$$\begin{aligned} \tau_c = w(p_2) &= \rho p_1 \{\sin\theta_c |\sin\theta| + \cos\theta_c \cos\theta\} \\ &= \rho p_1 \cos\{\theta_c - |\theta|\} = (\rho/c_1)\cos\{\theta_c - |\theta|\}, \end{aligned} \tag{0.74}$$

lies in the primary τ-domain. Thus, the deformation of Γ' in this case, must be a loop integral around τ_c as shown in Figure 0.4.

To see the advantage of using two complex planes in the Cagniard-de Hoop method, we note, as in the preceding example, that

$$\tau_s = \tau(p_s) = w(p_s, |x|, z) = \rho/c_1 > \tau_c = (\rho/c_1)\{\cos\theta_c - |\theta|\} = \tau_c, \tag{0.75}$$

and this identity holds no matter whether p_2 is in the primary p-domain or not. Again, note that τ_s is the maximum of τ for $0 < p < p_1$. Therefore, by just knowing the value of τ_c we cannot tell whether or not it lies between Γ' and S'. It is only when we see that it is the image of a point in the primary p-domain that we can be sure that it lies between these image contours. When p_2 is to the right of S, we know that

its image in the τ-domain lies on the second Riemann sheet of the branch point at τ_s and *not* between the image contours, Γ' and S'. However, by understanding the mapping from p to τ we readily know that for p_2 to the right of the primary p-domain, its image must be on the lower Riemann sheet with respect to the branch point at τ_s and at some $\tau < \tau_s$. Thus, such a choice of p_2 does not interfere with the deformation of Γ' onto S'.

We now have the machinery in place to find a time domain representation of the upward propagating wave for this problem in both the pre- and post-critical regions in Figure 0.3. We will discuss them in that order.

Case I: $|\theta| < \theta_c$.

From (0.69) and (0.72), it follows that in this case $p_s < p_2$ and the latter point is outside the primary p-domain. Therefore, its image is outside the primary τ-domain and the deformation from Γ' to S' proceeds unimpeded by the presence of the image τ_c of p_2. In analogy with the transformation from (0.51) to (0.57), in this case (0.67) becomes

$$u(x,z,s) = \frac{1}{4\pi i}\int_{\tau_s}^{\infty}\left[\frac{dp_+}{d\tau}\frac{R(p_+)}{\sqrt{p_1^2-p_+^2}} - \frac{dp_-}{d\tau}\frac{R(p_-)}{\sqrt{p_1^2-p_-^2}}\right]\exp\{-s\tau\}d\tau \tag{0.76}$$

and

$$U(x,z,t) = \mathrm{Im}\left\{\frac{dp_+}{d\tau}\frac{R(p_+)}{2\pi\sqrt{p_1^2-p_+^2}}\right\}H(t-\tau_s). \tag{0.77}$$

For this case, (0.63) is still valid, except that ρ is now defined by (0.69). Since the right side of this last expression is purely imaginary, we extract the imaginary part in (0.77) by choosing the real part of $R(p_+)$; that is,

$$U(x,z,t) = \frac{H(t-\rho/c_1)}{2\pi\sqrt{t^2-\rho^2/c_1^2}}\mathrm{Re}\{R(p_+)\}. \tag{0.78}$$

This result agrees with Aki and Richards, I, 1980, p. 230, eq. (6.57).

Case II: $\theta > \theta_c$.

In this case, as previously noted, $p_2 < p_s$ and lies in the primary p-domain, its image τ_c lies in the primary τ-domain and the deformed contour in the τ-domain is as shown in Figure 0.4. Consequently, we replace (0.76) by

$$\begin{aligned} u(x,z,s) &= \frac{1}{4\pi i}\int_{\tau_c}^{\tau_s} + \int_{\tau_s}^{\infty}\left[\frac{dp_+}{d\tau}\frac{R(p_+)}{\sqrt{p_1^2-p_+^2}} - \frac{dp_-}{d\tau}\frac{R(p_-)}{\sqrt{p_1^2-p_-^2}}\right]\exp\{-s\tau\}d\tau \\ &= u_1(x,z,s) + u_2(x,z,s), \end{aligned} \tag{0.79}$$

with u_1 and u_2 corresponding to the first and second integrals, respectively.

Let us first consider the integral $u_1(x,z,s)$ and its inverse transform $U_1(x,z,t)$. The fact that both limits of integration are finite tells us that the inverse transform is a function that "turns on" at $t = \tau_c$ and "turns off" at $t = \tau_s$. This finite interval of integration is the image of the line segment, $p_2 < p < p_s$ in the primary p-domain. On this interval, the change of variables defined in (0.68) is real. In analogy with (0.60) and (0.61), we find here that

$$\sqrt{p_1^2 - p^2} = \left[[2h-z]\tau + |x|\sqrt{p_1^2\rho^2 - \tau^2}\right]/\rho^2, \tag{0.80}$$

and

$$\frac{dp}{d\tau} = \frac{[2h-z]\tau + |x|\sqrt{p_1^2\rho^2-\tau^2}}{\rho^2\sqrt{p_1^2\rho^2-\tau^2}}, \tag{0.81}$$

with ρ defined by (0.69). Thus, we conclude that

$$\begin{aligned} U_1(x,z,t) &= \mathrm{Im}\left\{\frac{dp_+}{d\tau}\frac{R(p_+)}{2\pi\sqrt{p_1^2-\rho^2}}\right\}[H(t-\tau_c) - H(t-\tau_s)] \\ &= \frac{\mathrm{Im}\{R(p_+)\}}{2\pi}\frac{H(t-\tau_c)-H(t-\tau_s)}{\sqrt{\rho^2/c_1^2 - t^2}}. \end{aligned} \tag{0.82}$$

For $u_2(x,z,s)$, the path of integration is one for which the $p(\tau)$ is again complex valued with the derivative as in the above case $\theta < \theta_c$,

$$U_2(x,z,t) = \frac{H(t-\rho/c_1)}{2\pi\sqrt{t^2-\rho^2/c_1^2}}\mathrm{Re}\,\{R(p_+)\}. \tag{0.83}$$

These results agree with Aki and Richards, I, p. 234, eq. (6.58).

This completes the discussion of this elementary problem. It is typical of the type of analysis that is necessary when viewing the change of variables as a mapping from one complex plane to another.

Three-dimensional free space Green's function

We now consider

$$v(x,y,z,\omega) = -\frac{1}{8\pi^2 i}\int_{-\infty}^{\infty}\int_{-\infty}^{\infty}\frac{dk_1 dk_2 \exp\{i[k_1 x + k_2 y + \sqrt{\omega^2/c_1^2 - k_1^2 - k_2^2}|z|]\}}{\sqrt{\omega^2/c_1^2 - k_1^2 - k_2^2}}. \tag{0.84}$$

This is the three-dimensional analog of (0.49) and is of the form, (0.14), with $J = 1$ and

$$g(k_1,k_2,\omega) = -\frac{1}{8\pi^2 i}\frac{1}{\sqrt{\omega^2/c_1^2 - k_1^2 - k_2^2}} = -\frac{1}{8\pi^2 i\omega}\frac{1}{\sqrt{1/c_1^2 - k_1^2/\omega^2 - k_2^2/\omega^2}}, \tag{0.85}$$

so that in (0.15), $n = -1$.

The transformations below (0.15) can be applied here, leading to functions f and u defined by (0.21). That is,

$$f(p) = \frac{1}{8\pi^2 i}\frac{1}{\sqrt{1/c_1^2 + q^2 - p^2}} = \frac{1}{8\pi^2 i}\frac{1}{\sqrt{p_1^2 - p^2}} \tag{0.86}$$

and

$$v(x,y,z,is) = su(r,z,s). \tag{0.87}$$

In the first equation p_1 is defined by (0.22) and in the second equation, multiplication by s means that we must differentiate with respect to t in addition to integrating

with respect to q in order to obtain the time domain Green's function from the result of applying the Cagniard method to the function u.

With these results we find that we must analyze the integral representation

$$u(r,z,s) = \frac{1}{8\pi^2 i}\int_\Gamma \frac{dp}{\sqrt{p_1^2 - p^2}} \exp\{-sw(p,r,z)\}, \tag{0.88}$$

with w given by

$$w(p,r,z) = pr + \sqrt{p_1^2 - p^2}|z|,\ p_1^2 = 1/c_1^2 + q^2. \tag{0.89}$$

These equations are the same as (0.51) and (0.52) except for (i) replacement of x and $|x|$ by r and (ii) an extra factor of $1/2\pi$ in the definition of u. Thus, we read off the result of the Cagniard method from (0.64) as

$$U(r,z,t) = \frac{H(t-\rho/c_1)}{4\pi^2\sqrt{t^2 - \rho^2/c_1^2}},\quad \rho = \sqrt{r^2+z^2}. \tag{0.90}$$

Here we see the power of de Hoop's transformation: except for the quadrature and differentiation to follow, the application of the Cagniard method to the representation of the three dimensional Green's function is reduced to the analysis of the two-dimensional problem treated earlier.

As noted above, it is necessary to integrate this result with respect to q :

$$\begin{aligned}\int_{-\infty}^{\infty} U(r,z,t)dq &= \frac{H(t-\rho/c_1)}{4\pi^2\rho}\int_{-\sqrt{t^2-\rho^2/c_1^2}}^{\sqrt{t^2-\rho^2/c_1^2}} \frac{dq}{\sqrt{t^2 - \rho^2/c_1^2 - \rho^2 q^2}} \\ &= \frac{H(t-\rho/c_1)}{4\pi\rho}.\end{aligned} \tag{0.91}$$

Finally, we differentiate with respect to t to obtain v :

$$v(x,y,z,t) = \frac{\delta(t-\rho/c_1)}{4\pi\rho}. \tag{0.92}$$

In Chapter 5 of Cagniard's (1939, 1962) book and in Dix (1954), polar coordinates are used in the representation of the Green's function. This leads to a pair of integrals in transverse wave number and angle between the transverse wave vector and (x, y). The first of these integrals is treated by Cagniard's method. However, the function w depends on the polar angle, making the subsequent integration (the analog of the q integral here) much more difficult. This latter integration is a *tour de force* in complex function theory by those authors. The de Hoop transformations avoid this extremely difficult analysis, making application of his modification of Cagniard's method much more accessible and a method of choice for a broad class of problems.

The Sommerfeld Half-Plane Problem

We will consider here diffraction of a plane wave by a half-plane in the case where there is no equivalent causal problem. This is not a problem which is normally treated by the Cagniard-de Hoop method starting from the Laplace transform, because that method requires an equivalent causal problem for the (one-sided) Laplace transform to make sense. However, the structure of the problem certainly lends itself to treatment by the Cagniard-de Hoop method, if we start from a Fourier representation of the solution and carefully observe the interplay of singularities with the rotation of contour associated with the transformation from (k, ω) to (p, s).

The underlying problem is as follows. A plane acoustic wave in a constant density medium is incident from infinity on a half-plane occupying the region, $x > 0$, $z = 0$. The wave is also parallel to the y axis so that the problem is two-dimensional. Given a boundary condition, the objective is to find the total field everywhere. We will assume the boundary condition that the total field is zero on the scatterer.

In Figure 0.5, we show two possible directions of incident wave from above. The waves are distinguished by the relative inclination of the incidence direction, as defined

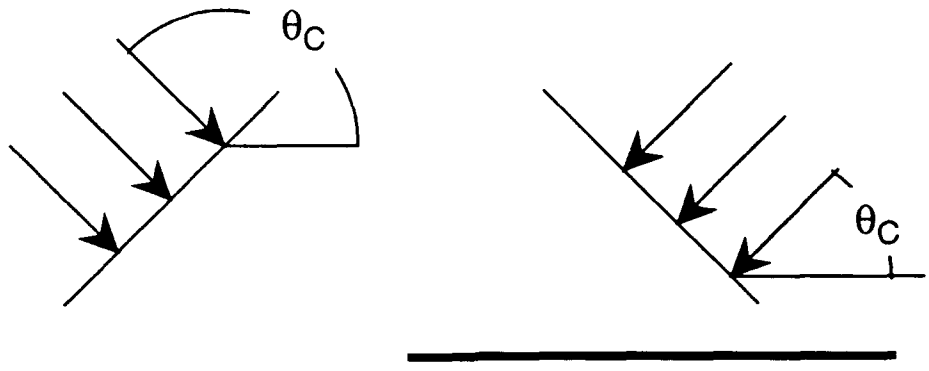

FIG. 0.5. Plane wave incident on a half-plane; two possible cases shown, distinguished by relative inclination to the scatterer. The angle of incidence is $\pi - \theta_c$.

by the angle $\pi - \theta_c$. For $\theta_c > \pi/2$—incidence from the left—one can easily construct an equivalent *initial value problem* starting with a plane wave initiated at some finite (negative) time. (This is equally true for a wave incident from the left and below. This is the case extensively treated in de Hoop [1958].) For $\theta_c < \pi/2$—incidence from the right—this is not so straightforward. For any finite negative time, the total field would have to include a plane wave terminated on the reflector plus its companion reflected wave, certainly more complicated than the "ideal" we propose to study. It will be seen below how the "noncausal" nature of the problem posed here for this latter choice of θ_c manifests itself in the analysis.

In the mathematical formulation, one begins by assuming an incident wave

$$v_I(x, z, \omega) = \exp\{-i\omega p_1[x\cos\theta_c + z\sin\theta_c]\},\ p_1 = 1/c_1, \tag{0.93}$$

with incidence angle

$$\theta_I = \pi - \theta_c. \tag{0.94}$$

Note that in this problem, we take z positive *upward* and we take θ to be the polar angle measured from the positive x axis. This interchanges the role of $\sin\theta$ and $\cos\theta$ from the standard geophysical convention. However, this makes comparison with other solutions in the literature easier, since this is Sommerfeld's notation.

The total solution is written as

$$v_T(x,z,\omega) = v_I(x,z,\omega) + v_S(x,z,\omega). \tag{0.95}$$

Here the scattered field $v_S(x,z,\omega)$ will include the reflected field, the diffracted field and *the negative of the incident field in the geometrical shadow.* With this formulation, $v_S(x,z,\omega)$ is an outward propagating wave for ω real. Alternatively, $v_S(x,z,\omega)$ must be an attenuating wave for $\mathrm{Im}\,\omega > 0$, or equivalently, $\mathrm{Re}\; s > 0$, which is where the type of Fourier transform we are considering here is initially defined.

The solution to this problem by the Weiner-Hopf technique (Carrier, Krook and Pearson, 1983) leads to the integral representation

$$v_S(x,z,\omega) = -\frac{\sqrt{\omega p_1(1-\cos\theta_c)}}{2\pi i}\int_{\Gamma_k} \frac{\exp\left\{i\left[kx + \sqrt{\omega^2 p_1^2 - k^2}|z|\right]\right\}}{[k+\omega p_1 \cos\theta_c]\sqrt{\omega^2 p_1^2 - k^2}}dk\ . \tag{0.96}$$

The contour Γ_k is shown in Figure 0.6 for the case $\mathrm{Re}\,\omega > 0$ and $\cos\theta_c > 0$. This is the case which is inherently noncausal.

Recall that part of our process of transformation from (k,ω) to (p,s) involved a rotation of ω from the real axis to the imaginary axis, albeit after rescaling k. In Figure 0.6, one can see that a rotation of ω will cause the pole to rotate *through* the path of integration. This is not acceptable, unless we account for the residue at the pole. If we were to rescale k, the singularities would lie on the axis; for $\mathrm{Im}\,\omega > 0$ the image contour would pass between them from upper left to lower right, and now the same difficulty would arise from further rotation of the contour with a fixed pole.

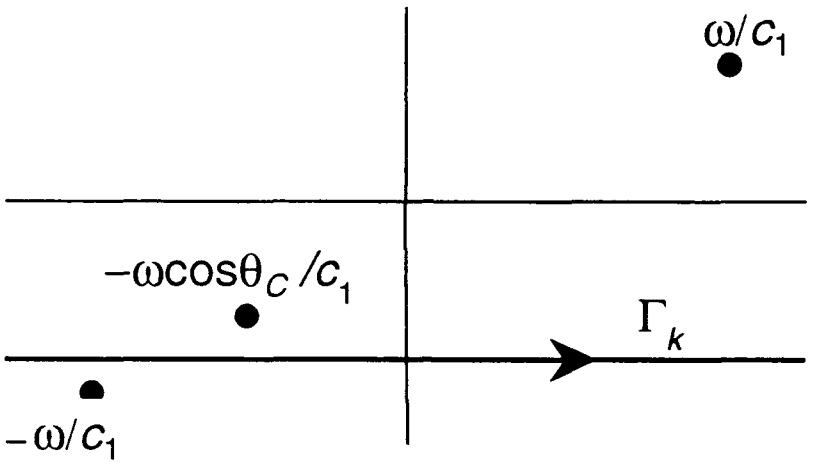

FIG. 0.6. The contour, Γ_k.

When $\cos\theta_c < 0$, the pole moves to the first quadrant, Γ_k can be replace by the Re k axis, and the pole rotates *away* from the contour along with the branch point in the first quadrant as $\arg\omega$ increases. Equivalently, after rescaling, $-k = \omega p$, the contour of integration would move away from all singularities with increasing α just as in the previous two examples. Recall that this is the case that corresponds to an equivalent causal problem and our analysis is no more difficult than it was for the standard problems treated by the Cagniard-de Hoop method. We proceed with the analysis of that more interesting case for which there is no equivalent causal problem, that is, for $\cos\theta_c > 0$.

Let us replace Γ_k in Figure 0.6 by the contour in Figure 0.7 and replace the integral over this contour by the sum of the residue at the pole and an integral along the real axis. That is,

$$v_S(x,z,\omega) = v_{RES}(x,z,\omega) + v(x,z,\omega),$$

$$v_{RES}(x,z,\omega) = -\exp\left\{i\omega p_1\left[-x\cos\theta_c + |z|\sin\theta_c\right]\right\}, \tag{0.97}$$

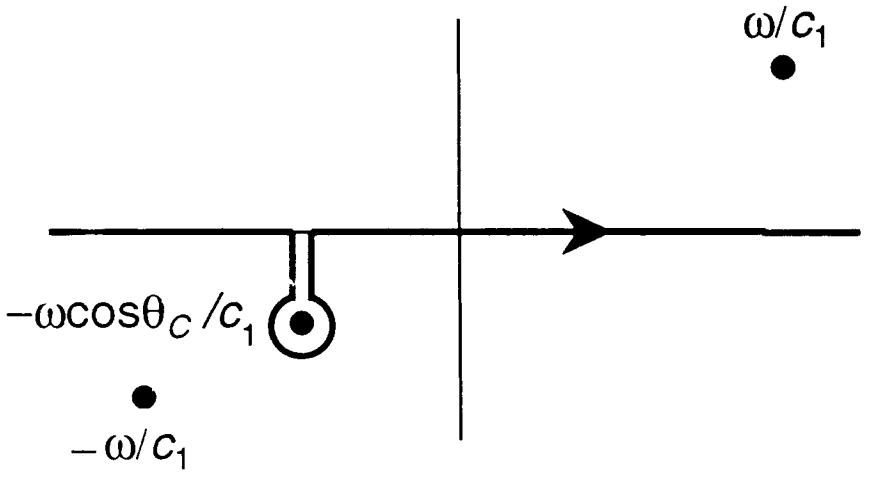

FIG. 0.7. Replacement contour for Γ_k.

$$v(x,z,\omega) = -\frac{\sqrt{\omega p_1(1-\cos\theta_c)}}{2\pi i}\int_{-\infty}^{\infty}\frac{\exp\left\{i\left[kx+\sqrt{\omega^2p_1^2-k^2}|z|\right]\right\}}{[k+\omega p_1\cos\theta_c]\sqrt{\omega p_1+k}}dk\ .$$

Now we can introduce the change of variables (0.20), $k = \omega p\,\mathrm{sgn}(x)$, carry out the rotation of ω to the imaginary axis, and set $\omega = is$ (as previously described) to obtain the standard form of the integral representation for $u(x,z,s) = v(x,z,is)$:

$$u(x,z,s) = \frac{\sqrt{(1-\cos\theta_c)}}{2\pi i\sqrt{c_1}}\int_\Gamma \frac{\exp\{-sw(p,|x|,z)\}}{[p\ \mathrm{sgn}(x)+p_1\cos\theta_c]\sqrt{p\mathrm{sgn}(x)+p_1}}dp\ . \qquad (0.98)$$

Again, in this equation,

$$w(p,|x|,z) = p|x| + \sqrt{p_1^2-p^2}|z|,\ p_1 = 1/c_1, \qquad (0.99)$$

and Γ is the contour of Figure 0.2.

This analysis could have started from an integral in which ω was real, with the contour Γ_k replaced by the contour shown in Figure 0.8. The final result would not change. The rotation of contour after rescaling k and rotation of ω or the rotation of ω first would produce exactly the same interplay between the contour of integration and the pole.

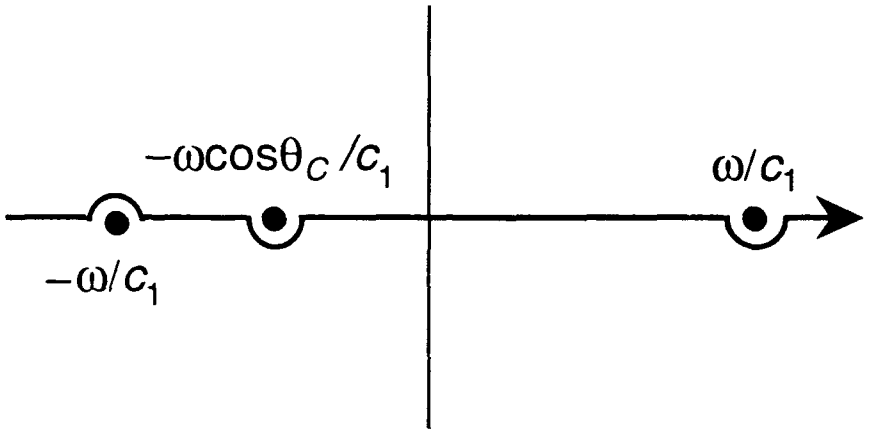

FIG. 0.8. Contour of integration for Reω.

We have now made the main point of this example concerning the Cagniard-de Hoop method, that the change of variables plus rotation implicit in the equation $\omega = is$, starting from ω (nearly) real and ending with s real, may introduce special contributions as a consequence of singularities forced to pass "through" the contour of integration.

It is interesting to continue the analysis of the solution via the Cagniard-de Hoop method and we proceed to do so, despite having already accomplished our main objective with respect to this problem.

We note first that, $v_{RES}(x,z,\omega)$ in (0.97) can also be written as

$$v_{RES}(x,z,\omega) = \begin{cases} -\exp\{i\omega p_1 [x\cos(\pi-\theta_c) + z\sin(\pi-\theta_c)]\}, & z > 0, \\ -\exp\{i\omega p_1 [x\cos(\pi+\theta_c) + z\sin(\pi+\theta_c)]\}, & z < 0. \end{cases} \tag{0.100}$$

The first line here has the form of the reflected wave, while the second line has the form of the negative of the incident wave. As previously noted, we are alert for such terms to appear in the solution v_S. The only problem is that these two expressions cover the entire upper and lower half-spaces, respectively, rather than the reflection region (labeled I in Figure 0.9) in the former case and the geometrical shadow (labeled

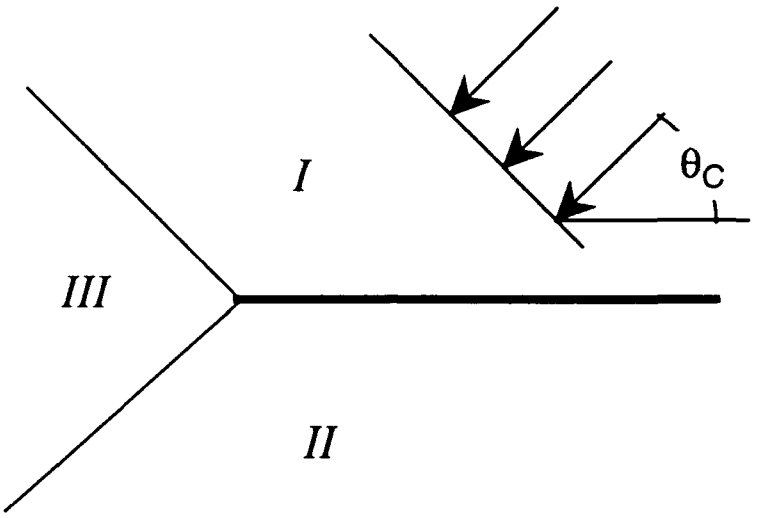

FIG. 0.9. Geometrical optics regions for the scattering of a plane wave by a half-plane reflector. Region I: geometrical reflection. Region II: geometrical shadow for the incident wave. Region III: remainder of the plane. v_{RES} extends the reflected and negative incidence fields, respectively, to Region III.

II in Figure 0.9) in the latter case. Thus, we must be alert to further corrections to these plane waves in the representation of $u(x, z, s)$ in (0.98).

We now turn to the analysis of $u(x, z, s)$ defined by (0.98). Because θ is measured from the x-axis in this example, the location of the saddle point in (0.34) is given by

$$p_s = p_1|\cos\theta| = \frac{|\cos\theta|}{c_1} = \frac{|x|}{c_1\rho}, \ \rho = \sqrt{x^2 + z^2}. \tag{0.101}$$

What is of interest to us here, is the interplay of the location of p_s and the pole of the integrand in (0.98). We note first that the pole is at some $p < 0$ for $x > 0$ and therefore is outside of the primary p-domain. Therefore, we need only consider the case $x < 0$ and the pole located at

$$p_p = -\text{sgn}(x)p_1\cos\theta_c = -\text{sgn}(x)\cos\theta_c/c_1. \tag{0.102}$$

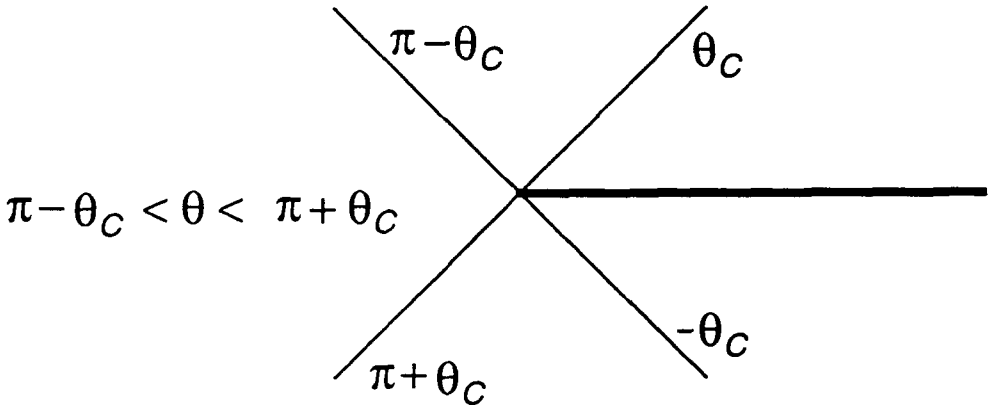

FIG. 0.10. The regions of incidence and reflection described in terms of angular boundaries.

In this case, it is at least necessary for x to be negative for the pole to be in the primary p-domain; that is,

$$x < 0 \;\Rightarrow\; \pi/2 < \theta < 3\pi/2,\; |\cos\theta| = -\cos\theta. \tag{0.103}$$

Furthermore, it is necessary for the pole to be to the left of the saddle point for it to be in the primary p-domain; that is,

$$p_p < p_s \;\Rightarrow\; \cos\theta_c < -\cos\theta = \cos(\pi - \theta). \tag{0.104}$$

When we rewrite this result in terms of angles,

$$-\theta_c < \pi - \theta < \theta_c \;\Rightarrow\; \pi - \theta_c < \theta < \pi + \theta_c, \tag{0.105}$$

we see that the pole is in the primary p-domain for (x, z) in Region III of Figure 0.9. See Figure 0.10.

For this angular range, the image of the pole is in the primary τ-domain and the deformation of Γ' is a loop integral starting at the pole just as in Figure 0.4. For the pole in the τ plane and the branch point at τ_s "well-separated," we can consider the two contributions separately. It is fairly straightforward to verify that

the residue at this pole is just the negative of the wavefields given in (0.100). That is, the residue at this pole has the effect of eliminating the reflected wave and the negative of the incident wave in the regions where we did not expect them to appear in the first place; now these waves are restricted to the region of reflection and to the geometrical shadow, respectively.

For (x, z) near the boundaries of Region III the pole and branch point are nearby one another. If we wish to allow them to coalesce, we cannot consider the contributions separately. In the limit of coalescence of the singularities we no longer have a simple residue plus branch cut integral and we must content ourselves with numerical integration or a uniformly valid asymptotic approximation that allows coalescence.

Let us suppose now that the pole and the saddle point are "well-separated," whether or not we are in Region III. We denote by $u_D(x, y, s)$ the contribution from the loop integral starting at the saddle point, the contour S' in Figure 0.2. This integral is obtained in the standard way, as described for the previous two examples, from the representation (0.98). That is,

$$u_D(x, z, s) = \frac{\sqrt{(1-\cos\theta_c)}}{2\pi i\sqrt{c_1}} \int_{S'} \frac{\exp\{-s\tau\}}{[p\mathrm{sgn}(x) + p_1\cos\theta_c]\sqrt{p\mathrm{sgn}(x) + p_1}} \frac{dp}{d\tau} d\tau \ . \quad (0.106)$$

Since w in (0.99) is the same as (0.52), the analysis of the first example can be used here, as well. In particular, $dp/d\tau$ is given by (0.61) and τ_s is given by (0.56). After some algebra, we find in analogy with (0.57) that

$$u_D(x, z, s) = \frac{\sqrt{(1-\cos\theta_c)}}{\pi i\sqrt{c_1}\rho^2} \int_{p_1\rho}^{\infty} \frac{e^{-s\tau}}{\sqrt{\tau^2 - p_1^2\rho^2}}$$

$$\cdot \mathrm{Re}\left\{ \frac{\tau|z| - i|x|\sqrt{\tau^2 - p_1^2\rho^2}}{[p_+(\tau)\mathrm{sgn}(x) + p_1\cos\theta_c]\sqrt{p_+(\tau)\mathrm{sgn}(x) + p_1}} \right\} d\tau. \quad (0.107)$$

In this equation, $p_+(\tau)$ is given by (0.62). From this result, the time-domain solution is given by

$$u_D(x,z,s) = \frac{\sqrt{(1-\cos\theta_c)}}{\pi i\sqrt{c_1}\rho^2}\frac{H(t-\rho/c_1}{\sqrt{\tau^2-1/c_1^2\rho^2}}$$

$$\cdot\mathrm{Re}\left\{\frac{\tau|z|-i|x|\sqrt{\tau^2-\rho^2/c_1^2}}{[p_+(\tau)\mathrm{sgn}(x)+\cos\theta_c/c_1]\sqrt{p_+(\tau)\mathrm{sgn}(x)+1/c_1}}\right\}. \quad (0.108)$$

This is the diffracted wave. It is a cylindrical wave radiating from the origin at time $t = 0$, which is the arrival time of the incident wave.

We have seen here the application of the Cagniard-de Hoop method to a "nontraditional" problem. The transformation from (k,ω) to (p,s) was seen to have a new feature—the interplay of the rotation of contour with a singularity (a pole) of the integrand. Also, for this problem, the body wave manifests itself through a pole of the integrand and the saddle point of $w(p,x,z)$ gave rise to the edge-diffracted wave. This is in contrast with layered-media problems where the saddle point gives rise to the body wave.

CONCLUSIONS

We have proposed an approach to the Cagniard method using a complex time domain. We have attempted to show that there are advantages to promoting the time domain to such "equal status" with the slowness domain. We avoid the usual folding of contour in the slowness domain because we also believe that there are advantages to having both endpoints of integration at infinity. Deformation of the original contour of integration onto the Cagniard path on which the exponent is real is equivalent to closing down the image contour in the τ-domain on the real axis. It was shown in this process that a particular saddle point and its associated paths of steepest ascent play a crucial role in the analysis. The original contour and the

contour made up of these two ascent paths define a primary p-domain whose image, the primary τ-domain, is central to the analysis of deformation of contour. Indeed, the pair of steepest ascent paths will always form the tails of the usual Cagniard paths in the p-domain and will make up those paths in their entirety when there are no other singularities of the integrand in the primary p-domain. When there are singularities in the primary p-domain, their images appear in the primary τ-domain and the closing down of the image contour around the real axis in that domain must take account of these singularities.

We have also addressed the problem of transforming an integral solution in the (k, ω) domain into an integral solution in the (p, s) domain. It was shown here that careful analysis allows us to address noncausal problems as well as the causal ones normally treated by starting with one-sided Laplace transforms.

ACKNOWLEDGMENTS

Financial support for this work was provided in part by the Office of Naval Research, Mathematics Division and by the United States Department of Energy, Grant Number DE-FG02-89ER14079. (This support does not constitute an endorsement by DOE of the views expressed in this paper.)

REFERENCES

Aki, K., and P. G. Richards, 1980, Quantitative Seismology: W. H. Freeman and Company, San Francisco

Bleistein, N., 1984, Asymptotic Expansions of Integrals: Academic Press, New York.

Cagniard, L., 1939, Réflexion et Réfraction des ondes Séismique Progressives: Gauthiers-Villars, Paris.

Cagniard, L., 1962, Reflection and Refraction of Progressive Seismic Waves: Trans. by E. A. Flinn and C. H. Dix, McGraw-Hill, New York.

Carrier, G. F., Krook, M., and Pearson, C. E., 1983, Functions of a Complex Variable: Hod Books, Ithaca, 438 pages.

Cisternas, A., Betancourt, O., and Leiva, A., 1973, Body waves in a "real earth": Bul. Seism. Soc. Am., 63, 145-156.

de Hoop, A. T., 1958, Representation theorems for the displacement in an elastic solid and their application to elastodynamic diffraction theory: PhD Thesis, Technische Hogeschool, Delft.

de Hoop, A. T., 1960, A modification of Cagniard's method for solving seismic pulse problems: Applied Science Research, B8, 349-356.

de Hoop, A. T., 1988, Tutorial: Large-offset approximations in the modified Cagniard method for computing synthetic seismograms: a survey: Geophysical Prospecting, 36, 5, 465-477.

Dix, C. H., 1954, The method of Cagniard in seismic pulse problems: Geophysics, XIX, 4, 722-738.

Garvin, W. W., 1956, Exact transient solution of the buried line source problem: Proc. Roy. Soc. London, A, 234, 528-541.

Levinson, N., and R. H. Redheffer, 1970, Complex Variables: Holden-Day, Inc., Oakland.

Sneddon, I. N., 1972, The Use of Integral Transforms: McGraw-Hill Book Company, New York.

Spencer, T. W., 1960: The method of generalized reflection and transmission coefficients: Geophysics, 25, 625-641.

van der Hijden, J. H. M. T., 1987, Propagation of Transient Elastic Waves in Stratified Anistropic Media: Elsevier Science Publishers, Amsterdam.

van der Waerden, B. L., 1951, On the method of saddle points: Appl. Sci. Res., B2, 33-45.

Widder, D. V., 1959, The Laplace Transform: 5th Edition, Princetion University Press, Princeton.

SECURITY CLASSIFICATION OF THIS PAGE

REPORT DOCUMENTATION PAGE

1a REPORT SECURITY CLASSIFICATION Unclassified	1b RESTRICTIVE MARKINGS None.
2a SECURITY CLASSIFICATION AUTHORITY	3 DISTRIBUTION/AVAILABILITY OF REPORT
2b DECLASSIFICATION/DOWNGRADING SCHEDULE	
4 PERFORMING ORGANIZATION REPORT NUMBER(S) CWP-098P	5 MONITORING ORGANIZATION REPORT NUMBER(S)
6a NAME OF PERFORMING ORGANIZATION Center for Wave Phenomena Colorado School of Mines 6b OFFICE SYMBOL (If applicable)	7a NAME OF MONITORING ORGANIZATION Mathematical Sciences Division
6c ADDRESS (City, State, and ZIP Code) Golden, CO 80401	7b ADDRESS (City, State, and ZIP Code) 800 N. Quincy Street Arlington, VA 22217-5000
8a NAME OF FUNDING/SPONSORING ORGANIZATION 8b OFFICE SYMBOL (If applicable)	9 PROCUREMENT INSTRUMENT IDENTIFICATION NUMBER N00014-91-J-1267
8c ADDRESS (City, State, and ZIP Code)	10 SOURCE OF FUNDING NUMBERS PROGRAM ELEMENT NO. / PROJECT NO. / TASK NO / WORK UNIT ACCESSION NO.

11 TITLE (Include Security Classification)
The Cagniard Method in Complex Time Revisited

12 PERSONAL AUTHOR(S)
Norman Bleistein and Jack K. Cohen

13a TYPE OF REPORT	13b TIME COVERED	14 DATE OF REPORT (Year, Month, Day)	15 PAGE COUNT
Technical	FROM 10/1/90 TO 9/30/91	4/4/91	46

16 SUPPLEMENTARY NOTATION
Submitted for publication in Geophysical Prospecting

17 COSATI CODES			18 SUBJECT TERMS (Continue on reverse if necessary and identify by block number)
FIELD	GROUP	SUB-GROUP	Cagniard-deHoop, conformal mapping, Laplace transform, stratified media, method of steepest descent

19 ABSTRACT (Continue on reverse if necessary and identify by block number)

See Reverse.

Statement A per telecon Dr. Lau
ONR/Code 1111MA
Arlington, VA 22217-5000

NWW 10/2/91

20 DISTRIBUTION/AVAILABILITY OF ABSTRACT	21 ABSTRACT SECURITY CLASSIFICATION
☒ UNCLASSIFIED/UNLIMITED ☐ SAME AS RPT ☐ DTIC USERS	

22a NAME OF RESPONSIBLE INDIVIDUAL	22b TELEPHONE (Include Area Code)	22c OFFICE SYMBOL
Norman Bleistein	303 273-3557	

Abstract

The Cagniard-de Hoop method is ideally suited to the analysis of wave propagation problems in stratified media. The method applies to the integral transform representation of the solution in the transform variables (s,p) dual of the time and transverse distance. The objective of the method is to make the p-integral take the form of a forward Laplace transform, so that the cascade of the two integrals can be identified as a forward and inverse transform, thereby making the actual integration unnecessary. That is, the exponent, $-sw(p)$ is set equal to $-s\tau$, with τ varying from some (real) finite time to infinity. As usually presented, the p-integral is deformed onto a contour on which the exponent is real and decreases to $-\infty$ as p goes to infinity. We have found that it is often easier to introduce a complex variable τ for the exponent and carry out the deformation of contour in the complex τ-domain.

Typically, the method is applied to an integral that represents one body wave plus other types of waves. In this approach, the saddle point of $w(p)$ that produces the body wave plays a crucial role because it is *always* a branch point of the integrand in the τ-domain integral. Furthermore, the paths of steepest *ascent* from the saddlepoint are always the tails of the Cagniard path along which $w(p) \rightarrow \infty$.

This approach to the Cagniard-de Hoop method represents a return from de Hoop's modification to Cagniard's original method, but with simplifications that make the original method more tractable and straightforward. This approach is also reminiscent of van der Waerden's approach to the method of steepest descents, which starts exactly the same way.